ACS Medicinal Chemistry Letters

Letter

pubs.acs.org/acsmedchemlett

Structure–Activity Relationships and Molecular Modeling of 1,2,4-Triazoles as Adenosine Receptor Antagonists

Jens Carlsson,*[,†] Dilip K. Tosh,[‡] Khai Phan,[‡] Zhan-Guo Gao,[‡] and Kenneth A. Jacobson*[,‡]

[†]Center for Biomembrane Research, Department of Biochemistry and Biophysics, Stockholm University, SE-10691 Stockholm, Sweden

[‡]Molecular Recognition Section, Laboratory of Bioorganic Chemistry, National Institute of Diabetes and Digestive and Kidney Diseases, National Institutes of Health, Bethesda, Maryland 20892, United States

Supporting Information

ABSTRACT: The structure–activity relationship (SAR) for a novel class of 1,2,4-triazole antagonists of the human A_{2A} adenosine receptor ($hA_{2A}AR$) was explored. Thirty-three analogs of a ligand that was discovered in a structure-based virtual screen against the $hA_{2A}AR$ were tested in hA_1, A_{2A}, and A_3 radioligand binding assays and in functional assays for the $A_{2B}AR$ subtype. As a series of closely related analogs of the initial lead, **1**, did not display improved binding affinity or selectivity, molecular docking was used to guide the selection of more distantly related molecules. This resulted in the discovery of **32**, a $hA_{2A}AR$ antagonist (K_i 200 nM) with high ligand efficiency. In light of the SAR for the 1,2,4-triazole scaffold, we also investigated the binding mode of these compounds based on docking to several $A_{2A}AR$ crystal structures.

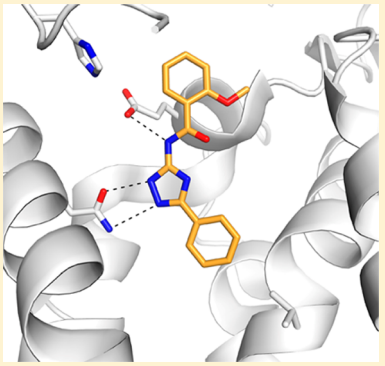

KEYWORDS: *1,2,4-Triazole, A_{2A} adenosine receptor, antagonist, molecular docking, structure–activity relationship*

Extracellular adenosine regulates numerous physiological processes via activation of four G protein-coupled receptors (GPCRs).[1] The A_1, A_{2A}, A_{2B}, and A_3 adenosine receptor (AR) subtypes display varying affinities for adenosine and act via different signaling pathways. The A_{2A} and $A_{2B}AR$ subtypes are primarily coupled to G_s and thereby increase intracellular cAMP levels, whereas the A_1 and A_3ARs inhibit cAMP production via activation of G_i. The human (h) $A_{2A}AR$ is expressed in both the periphery and the central nervous system (CNS). The extracellular adenosine concentration increases in response to cell stress or damage, and activation of the $hA_{2A}AR$ protects tissues by reducing inflammation.[2] In the CNS, a postsynaptic striatal $hA_{2A}AR$ regulates the effects of other neurotransmitters via interactions with D_2 dopamine receptors and metabotropic glutamate receptor-5.[3] There is a growing interest in the $hA_{2A}AR$ as a drug target. Agonists are explored as anti-inflammatory drugs, and antagonists are developed for the treatment of neurodegenerative disorders such as Parkinson's disease.[4,5]

Until recently, drug discovery efforts targeting the $hA_{2A}AR$ have been limited to ligand-based medicinal chemistry approaches.[6,7] Many compound series that display high affinity for the A_{2A} subtype have been developed based on adenosine or naturally occurring antagonists, e.g. caffeine.[8] In late 2008, the determination of the first atomic-resolution structures of the $hA_{2A}AR$[9] led to an increasing interest in the use of structure-based approaches in ligand discovery. One of these, the molecular docking method, can be used to computationally screen large chemical libraries against the binding site of a protein.[10] Two independent docking screens that were carried out against the first crystal structure of the $hA_{2A}AR$ were remarkably successful, with hit-rates of 35 and 41%, respectively.[11,12]

The starting point of this study, compound **1**, was discovered based on a docking screen of 1.4 million compounds against the first high-resolution crystal structure of the $hA_{2A}AR$ (Table 1, Figure 1A). The molecule was ranked as number 88 based on its score for complementarity to the orthosteric site and was selected for experimental evaluation together with 19 other compounds from the *in silico* screen. Seven of these molecules were shown to bind to the $A_{2A}AR$ with inhibition constant (K_i) values lower than 10 μM. Among these, compound **1** was one of the most potent and represented a novel class of 1,2,4-triazole antagonists.[11] Herein we explore the structure–activity relationship (SAR) for 1,2,4-triazole antagonists by testing a series of 33 analogs of **1** in radioligand binding assays against the A_1, A_{2A}, and A_3AR subtypes and functional assays for the A_{2B} receptor. Molecular docking to $hA_{2A}AR$ receptor crystal structures (PDB accession codes 3eml[9] and 3pwh[13]) was used to guide the selection of compounds for experimental testing and to investigate the binding modes of the ligands.

Received: April 20, 2012
Accepted: July 29, 2012
Published: July 30, 2012

Table 1. Binding Affinities of a Series of 1,2,4-Triazole Derivatives at the Human A_1, A_{2A}, and A_3ARs Measured in Radioligand Binding Assays and Percent Inhibition of cAMP Accumulation in the Presence of 300 nM NECA in a Functional Assay for the A_{2B}AR

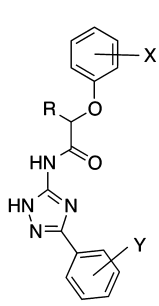

(1-14,18-23)

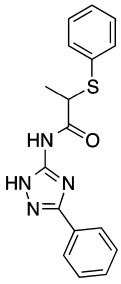

(15)

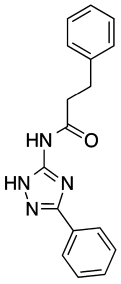

(16)

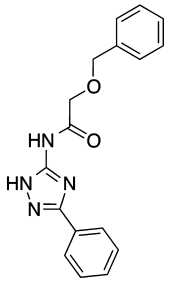

(17)

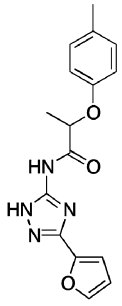

(24)

				K_i (μM) or *% inhibition at 10 μM*[a]			
compd	R	X	Y	A_1	A_{2A}	A_3	A_{2B}
1	CH_3	3-CH_3	H	*19%*	1.2 ± 0.1	3.0 ± 0.2	*18%*
2	CH_3	3-Cl	H	1.1 ± 0.1	1.0 ± 0.2	2.6 ± 0.5	*28%*
3	CH_3	H	H	5.2 ± 0.8	1.0 ± 0.1	3.3 ± 0.6	*23%*
4	CH_3	4-CH_3	H	*38%*	6.4 ± 0.9	1.4 ± 0.2	*−6%*
5	CH_3	4-Cl	H	3.9 ± 0.4	4.0 ± 0.9	2.5 ± 0.1	*51%*
6	CH_3	2-F	H	3.7 ± 0.4	1.0 ± 0.2	2.6 ± 0.7	*31%*
7	$(CH_3)_2$	4-Cl	H	*41%*	8.8 ± 0.6	0.5 ± 0.1	*6%*
8	CH_2CH_3	H	H	1.5 ± 0.5	1.4 ± 0.2	1.9 ± 0.3	*−9%*
9	H	3-CH_3	H	2.3 ± 0.7	2.0 ± 0.4	1.5 ± 0.3	*8%*
10	H	H	H	*20%*	1.8 ± 0.5	2.3 ± 0.1	*16%*
11	H	2-CH_3	H	*16%*	1.7 ± 0.3	1.0 ± 0.1	*13%*
12	H	2,6-CH_3	H	*49%*	1.7 ± 0.5	5.5 ± 0.3	*43%*
13	H	3-$(CH_2)_3$-4	H	*46%*	3.9 ± 0.2	2.2 ± 0.8	*9%*
14	H	3,5-CH_3	H	1.6 ± 0.7	3.2 ± 0.8	2.7 ± 0.9	*−5%*
15				3.3 ± 0.9	2.2 ± 1.0	1.9 ± 0.2	*21%*
16				*40%*	3.4 ± 0.7	8.3 ± 0.6	*40%*
17				8.1 ± 0.7	5.0 ± 0.1	4.6 ± 0.9	*7%*
18	H	H	4-F	*2%*	3.5 ± 0.6	1.5 ± 0.3	*−10%*
19	H	2-F	4-CH_3	*2%*	*2%*	*50%*	*11%*
20	H	2-OCH_3	4-CH_3	*8%*	*49%*	1.0 ± 0.1	*−10%*
21	H	H	4-CH_3	6.5 ± 1.5	3.6 ± 0.4	3.2 ± 0.4	*23%*
22	CH_3	H	2-CH_3	*6%*	*26%*	*48%*	*−3%*
23a	CH_3	H	3-CH_3	8%	2.0 ± 0.1	5.9 ± 1.2	*5%*
23b	CH_3 (*R*)	H	3-CH_3	*12%*	1.8 ± 0.3	6.3 ± 1.4	
23c	CH_3 (*S*)	H	3-CH_3	*13%*	*23%*	*32%*	
24				*37%*	*38%*	5.3 ± 1.5	*−15%*

[a]Measured in three independent experiments.

A series of closely related derivatives of compound **1** was first tested to obtain an SAR that could serve as a starting point for further structural optimization (Table 1, compounds **1**−**24**). Compound **1** displayed a K_i of 1.2 μM in binding to the hA_{2A}AR. This differed from that reported previously by a factor of 6,[11] which was likely due to differences in the experimental conditions. Replacing the 3-methyl group on the phenoxy ring of compound **1** with either a chloride or hydrogen (**2** and **3**, respectively) did not change hA_{2A}AR affinity, while para-substituted compounds displayed 3−5-fold reductions of the binding affinity (**4**−**5**). Modifications at the chiral center did not improve affinity in the series (**7**−**8**). The 1,2,4-triazole scaffold was further explored starting from compound **9**, which lacked the chiral center of compound **1** and displayed a K_i of 2 μM at the hA_{2A}AR. Mono- and dimethyl substitutions on the phenoxy ring (**10**−**14**) did not significantly improve the affinity. In agreement with observations for compounds **2**−**5**, ortho and meta substitutions on the phenoxy ring did not affect binding, while para-substitutions led to a 2-fold loss of affinity. Replacing the phenoxy group with a phenylsulfanyl, benzyl, or benzyloxy group (**15**−**17**) led to 2−4-fold reductions of affinity compared to compound **1**. The predicted binding mode of compound **1** (Figure 1A) suggested that the phenoxy group interacted with residues in the extracellular loops (ELs). Although several residues in EL2 have been shown to be critical for ligand binding to the hA_{2A}AR,[14,15] the inherent flexibility of the GPCR loop regions makes it difficult to relate the SAR to the predicted binding modes for these analogs, a point to be discussed below. In the next step, substitutions on the 3-phenyl of the triazole ring were tested. Methyl substitutions in the para (**19**−**21**) and ortho (**22**) positions reduced hA_{2A}AR affinity, while the meta-methylated analog (**23a**) displayed a K_i of 2 μM. The reduction of affinity observed for all compounds with substitutions on the 3-phenyl ring suggested that this part of

dx.doi.org/10.1021/ml300097g | *ACS Med. Chem. Lett.* 2012, 3, 715−720

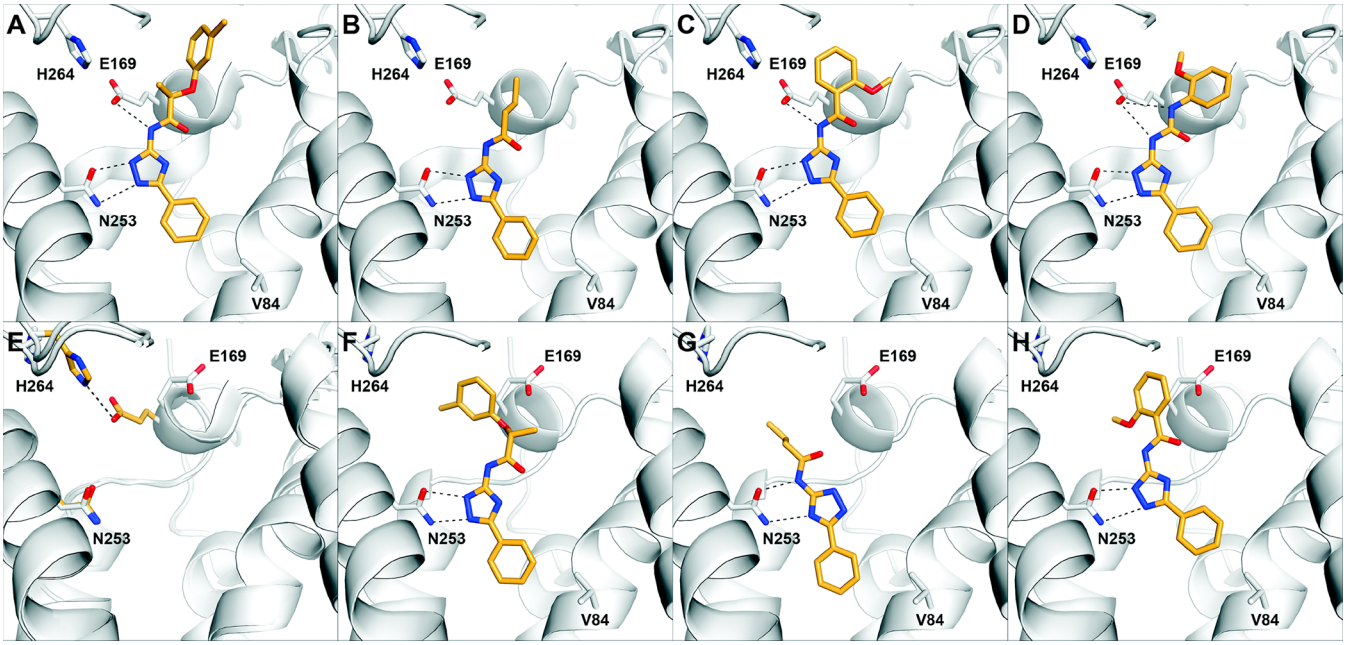

Figure 1. (A–D) Predicted binding modes for the A_{2A}AR crystal structure with PDB accession code 3eml: (A) **1**, (B) **27**, (C) **32**, (D) **33**. (E) Alignment of two A_{2A}AR crystal structures, PDB accession codes 3eml and 3pwh. Key residues are shown in sticks (orange, 3eml; white, 3pwh). (F–H) Predicted binding modes for the A_{2A}AR crystal structure with PDB accession code 3pwh: (F) **1**, (G) **27**, (H) **32**. The binding site is shown in white ribbons with selected side chains shown in sticks. Ligands are depicted with orange carbon atoms. Black dotted lines indicate hydrogen bonds.

Table 2. Binding Affinities of a Series of 1,2,4-Triazole Derivatives at the Human A_1, A_{2A}, and A_3ARs Measured in Radioligand Binding Assays and Percent Inhibition of cAMP Accumulation in the Presence of 300 nM NECA in a Functional Assay for the A_{2B}AR

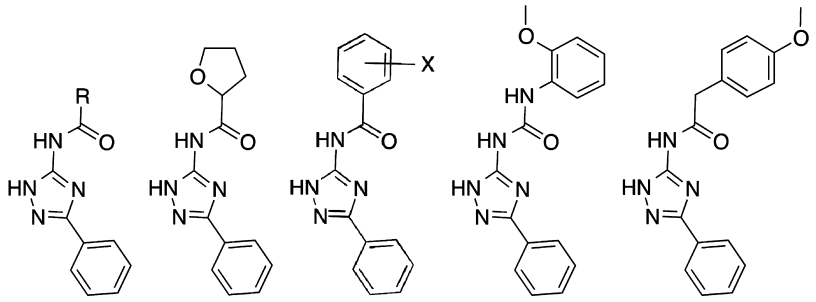

(25-27) 28 (29-32) (33) (34)

		K_i (μM) or % inhibition at 10 μM[a]			
compd	R	A_1	A_{2A}	A_3	A_{2B}
25	CH_3	*18%*	*43%*	0.3 ± 0.01	*10%*
26	CH_2CH_3	*39%*	2.5 ± 0.6	0.3 ± 0.2	*8%*
27	$(CH_2)_2CH_3$	0.8 ± 0.2	1.1 ± 0.2	0.2 ± 0.04	*5%*
28		3.2 ± 0.7	5.9 ± 0.5	3.1 ± 0.7	*−7%*
	X				
29	H	1.9 ± 0.3	0.4 ± 0.02	0.3 ± 0.2	*72%*
30	4-CH_3	1.3 ± 0.4	0.3 ± 0.1	0.1 ± 0.04	*29%*
31	4-Cl	*31%*	2.8 ± 0.8	0.2 ± 0.1	*−2%*
32	2-OCH_3	0.5 ± 0.1	0.2 ± 0.06	0.6 ± 0.2	*16%*
33		*22%*	0.2 ± 0.04	0.3 ± 0.2	*10%*
34		*29%*	1.0 ± 0.2	1.0 ± 0.3	*−6%*

[a]Measured in three independent experiments.

the ligand was buried in a sterically limited pocket, consistent with the predicted binding mode of compound **1**. Docking of compounds **1** and **19** suggested that a para substituent clashed with Val84 at the bottom of the orthosteric site (Figure 1A). This would push compound **19** upward toward the extracellular side and reduce favorable hydrogen bond interactions with Asn253. To test the possible benefit of a smaller substituent, the 3-phenyl was replaced with a furyl ring (**24**), but this led to

dx.doi.org/10.1021/ml300097g | ACS Med. Chem. Lett. 2012, 3, 715–720

reduced binding affinity. A possible reason for the loss of activity for compound **24** is that the smaller size of the furyl ring leads to a loss of van der Waals interactions in the orthosteric site. As the initial hit and several analogs were chiral (**1**−**6**, **8**, **15**, **22**, **23a**−**c**, **24**), the pure enantiomers (**23b** and **23c**) were synthesized for compound **23a**. This revealed that the active form of these ligands is the *R*-form, which is consistent with the docking predictions for both compound **23** and the initial hit in ref 11 (**1**, Figure 1A).

As the 23 close analogs of compound **1** did not display improved affinity, focus was placed on exploring more distantly related molecules. In this step, molecular docking calculations with DOCK3.6[16−18] were used to guide selection of molecules from commercially available libraries. Docking of compounds **1**−**24** to the $hA_{2A}AR$ crystal structure revealed that the phenoxy group was solvent exposed in several cases, and this conclusion was also supported by the affinity of several analogs being unaffected by substitutions of the phenyl ring. Based on these observations, it appeared likely that the phenoxy group did not contribute significantly to binding. To test this hypothesis, we explored compounds where the phenoxy group was replaced by a series of small aliphatic substituents (**25**−**28**). The ethyl- and propyl-substituted compounds displayed the same levels of affinity as the close analogs of compound **1**, confirming our prediction that the phenoxy group was not essential for binding (Table 2). The propyl substituted compound (**27**) displayed a K_i of 1.3 μM at the $A_{2A}AR$, which was equipotent to compound **1** (Figure 1B). However, it should be noted that **27** was significantly smaller than compound **1**, making it a more promising lead structure. The ligand efficiency (LE)[19] of compound **27**, calculated as its free energy of binding divided by the number of heavy atoms of the molecule, was 0.48, which put this fragment-sized compound in a promising range for further optimization.[20] In comparison, compound **1** displayed essentially the same affinity, but had a ligand efficiency of only 0.34 per atom.

To explore the possibility to further improve affinity while retaining relatively high ligand efficiency, another series of commercially available analogues was docked to the $hA_{2A}AR$ orthosteric binding site. A set of compounds with substituted phenyl rings that docked in the same overall binding mode as the other ligands was identified (Table 2, **29**−**34**). Compared to compound **1**, the molecules had a more compact structure and did not extend as far toward the ELs. Compound **29** displayed a K_i of 0.4 μM, a 3-fold improvement compared to **27**. This compound also retained a good LE of 0.44. A series of substitutions at the benzamide ring was explored, and the 2-methoxy substituted analog (**32**) led to another 2-fold improvement of affinity to a K_i of 200 nM (Figure 1C). Interestingly, replacing the amide of **32** with a urea group resulted in compound **33**, which also displayed a K_i of 200 nM at the $A_{2A}AR$ (Figure 1D).

In parallel to our efforts to identify a potent 1,2,4-triazole antagonist of the $hA_{2A}AR$, the 34 compounds were also screened at the hA_1, A_3, and $A_{2B}AR$ subtypes. Compound **1** was quite selective for the hA_{2A} and A_3AR with only 19% inhibition of A_1AR radioligand binding at 10 μM. The functional assays carried out for the $A_{2B}AR$ subtype showed no significant activity for compound **1** or any of the close analogs (Table 1). An unusual property of compounds **1**−**24** was that most of them bound with affinities in the 1−5 μM range at the A_{2A} and A_3AR subtypes, but 14 of them had ≤50% inhibition of the A_1AR at 10 μM. Based on sequence identity in the binding pocket, one would expect similar affinities for the A_1 and A_{2A} subtypes; the binding sites of the A_1 and A_{2A} subtypes differ by only a few residues in the orthosteric site, while 10 out of 20 binding cavity residues are unique to the A_3 receptor.[21] Based on a comparison of the $A_{2A}AR$ crystal structure to models of the A_1 and A_3 subtypes, we identified that Leu167 in EL2 (Glu and Gln in A_1 and A_3, respectively) and Met270 in helix 7 (Thr and Val in A_1 and A_3, respectively) were likely responsible for the observed A_{2A} and A_1 selectivity. The 1,2,4-triazole series was predicted to mainly have nonpolar interactions with Leu167 and Met270 in the $A_{2A}AR$, and in both cases, the most polar residue in this position is found in the A_1 subtype, which may reduce binding to this receptor (Figure S1, Supporting Information). As the size of the ligands was reduced, affinities typically increased at all subtypes for several of the most potent compounds (e.g., compounds **27**, **30**, and **32**). To further improve $A_{2A}AR$ selectivity, it is likely necessary to increase the compound size and extend substituents further toward nonconserved residues in the outer regions of the orthosteric site.

Subsequent to the testing of the 34 compounds described here, several new high-resolution structures of the $A_{2A}AR$ have been reported.[13] Interestingly, two of these are cocrystallized with the same antagonist, but the orientations of the ligand and residues in the ELs differ. Since the docking screen was carried out against a rigid receptor structure, the structural reorganization at the opening of the orthosteric site could significantly affect the predicted binding modes of the ligands. For this reason, representative ligands in the series were docked to an alternative crystal structure of the $A_{2A}AR$ (PDB accession code 3pwh[13]) to further investigate the binding mode of the 1,2,4-triazole antagonists. Docking to the first $hA_{2A}AR$ crystal structure (PDB accession code 3eml[14]) favored a conformation where the 1,2,4-triazole and amide nitrogens hydrogen bonded to Asn253 and Glu169, respectively (Figure 1A). In the alternative antagonist-bound crystal structure (PDB accession code 3pwh[13]), a hydrogen bond between the side chains of Glu169 and His264 was broken, which opened a hydrophobic pocket (Figure 1E). The predicted binding modes for three representative compounds to the alternative crystal structure are shown in Figure 1F−H. Compounds **1** and **32** were predicted to bind in the same overall binding mode in both structures, but compound **27** docked in an alternative conformation. In the case of compound **27**, the amide nitrogen interacts directly with Asn253 instead of Glu169, and an internal hydrogen bond was formed between the triazole ring and the amide carbonyl (Figure 1G). This binding mode was not accessible in the crystal structure used in the docking screen, because the ligands would clash with Glu169 in EL2. To test if this second binding mode was also energetically favored for **1** and **32**, docking calculations with restricted conformational sampling parameters were carried out for these two compounds. Both compounds **1** and **32** did fit in the alternative conformation (Figure 2). However, the docking energy of the alternative conformation was less favorable by more than 7 kcal/mol, in support of the first binding mode. The docking energies also tend to favor the first crystal structure (PDB accession code 3eml[9]) because of the strong electrostatic interaction energy between the ligands and Glu169. However, because the internal energy contribution of a receptor is notoriously difficult to estimate and is not taken into account in the docking energy calculations, the relative free energy of binding for the two conformations could not be calculated

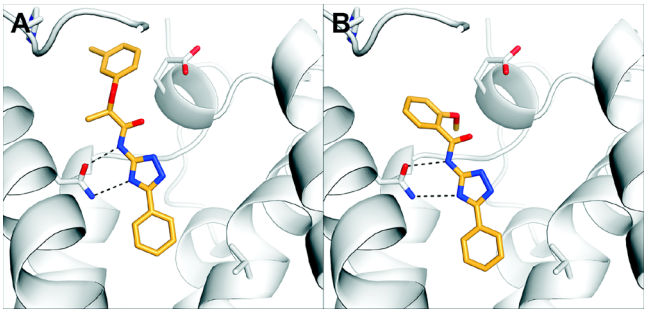

Figure 2. Alternative binding modes of compounds (A) **1** and (B) **32** to the A_{2A}AR crystal structure with PDB accession code 3pwh. The A_{2A}AR binding site is shown in white ribbons with selected side chains shown in sticks. Ligands are depicted with orange carbon atoms. Black dotted lines indicate hydrogen bonds.

accurately. Thus, it was not possible to conclude if only one, or both, receptor conformations were accessible for the 1,2,4-triazole series. In the case of the most potent 1,2,4-triazole ligand, compound **32**, both predicted binding modes appeared reasonable. In the first structure, the methoxy-substituent potentially could form hydrogen bonds with two backbone nitrogens in EL2 (Figure 1C), and in the alternative structure (Figure 1H), the same group was buried in a hydrophobic pocket created by the conformational reorganization. For this reason, it is likely advantageous to use an ensemble of crystal structures in lead optimization to identify the receptor conformation(s) that are most relevant for a given ligand of interest.

The present study explores the SAR for a novel class of 1,2,4-triazole antagonists. None of the close analogs of the initial hit, **1**, displayed improved potency at the hA_{2A}AR, but molecular docking calculations were used here to interpret the SAR and guide the selection of more distantly related compounds for experimental testing. This led to the discovery of compound **32**, with a K_i of 200 nM and a more favorable ligand efficiency of 0.42. The molecular docking calculations highlighted the need to consider several receptor conformations in lead optimization, which will help to guide further development of the 1,2,4-triazole series.

■ ASSOCIATED CONTENT

Ⓢ Supporting Information

Descriptions of the molecular modeling and experimental procedures. This material is available free of charge via the Internet at http://pubs.acs.org.

■ AUTHOR INFORMATION

Corresponding Author

*J.C.: phone, +46-8-16-4672; e-mail, jens.carlsson@dbb.su.se. K.A.J.: phone, +1-301-496-9024; fax, +1-301-480-8422; e-mail, kajacobs@helix.nih.gov.

Author Contributions

J.C. performed the molecular modeling studies. D.K.T., K.P., and Z.-G.G. carried out the experiments. The manuscript was written by J.C. and K.A.J.

Funding

Supported by the NIDDK Intramural Res. Program (to K.A.J.) and the Knut and Alice Wallenberg Foundation (to J.C.).

Notes

The authors declare no competing financial interest.

■ ABBREVIATIONS

AR, adenosine receptor; CNS, Central Nervous System; EL, extracellular loop; GPCR, G protein-coupled Receptor; LE, ligand efficiency; SAR, Structure−Activity Relationship

■ REFERENCES

(1) Fredholm, B. B.; IJzerman, A. P.; Jacobson, K. A.; Linden, J.; Müller, C. E. International Union of Basic and Clinical Pharmacology. LXXXI. Nomenclature and Classification of Adenosine Receptors-An Update. *Pharmacol. Rev.* **2011**, *63*, 1−34.

(2) Blackburn, M. R.; Vance, C. O.; Morschl, E.; Wilson, C. N. Adenosine receptors and inflammation. *Handb. Exp. Pharmacol.* **2009**, 215−69.

(3) Sebastiao, A. M.; Ribeiro, J. A. Adenosine receptors and the central nervous system. *Handb. Exp. Pharmacol.* **2009**, 471−534.

(4) Jacobson, K. A.; Gao, Z. G. Adenosine receptors as therapeutic targets. *Nat. Rev. Drug Discovery* **2006**, *5*, 247−264.

(5) Müller, C. E.; Jacobson, K. A. Recent developments in adenosine receptor ligands and their potential as novel drugs. *Biochim. Biophys. Acta, Biomembr.* **2011**, *1808*, 1290−1308.

(6) Costanzi, S.; Tikhonova, I. G.; Harden, T. K.; Jacobson, K. A. Ligand and structure-based methodologies for the prediction of the activity of G protein-coupled receptor ligands. *J. Comput.-Aided Mol. Des.* **2009**, *23*, 747−754.

(7) van der Horst, E.; van der Pijl, R.; Mulder-Krieger, T.; Bender, A.; IJzerman, A. P. Substructure-Based Virtual Screening for Adenosine A_{2A} Receptor Ligands. *ChemMedChem* **2011**, *6*, 2302−2311.

(8) Cristalli, G.; Muller, C. E.; Volpini, R. Recent developments in adenosine A_{2A} receptor ligands. *Handb. Exp. Pharmacol.* **2009**, 59−98.

(9) Jaakola, V. P.; Griffith, M. T.; Hanson, M. A.; Cherezov, V.; Chien, E. Y. T.; Lane, J. R.; IJzerman, A. P.; Stevens, R. C. The 2.6 Angstrom Crystal Structure of a Human A_{2A} Adenosine Receptor Bound to an Antagonist. *Science* **2008**, *322*, 1211−1217.

(10) Kitchen, D. B.; Decornez, H.; Furr, J. R.; Bajorath, J. Docking and scoring in virtual screening for drug discovery: Methods and applications. *Nat. Rev. Drug Discovery* **2004**, *3*, 935−949.

(11) Carlsson, J.; Yoo, L.; Gao, Z. G.; Irwin, J. J.; Shoichet, B. K.; Jacobson, K. A. Structure-Based Discovery of A_{2A} Adenosine Receptor Ligands. *J. Med. Chem.* **2010**, *53*, 3748−3755.

(12) Katritch, V.; Jaakola, V. P.; Lane, J. R.; Lin, J.; IJzerman, A. P.; Yeager, M.; Kufareva, I.; Stevens, R. C.; Abagyan, R. Structure-Based Discovery of Novel Chemotypes for Adenosine A_{2A} Receptor Antagonists. *J. Med. Chem.* **2010**, *53*, 1799−1809.

(13) Doré, A. S.; Robertson, N.; Errey, J. C.; Ng, I.; Hollenstein, K.; Tehan, B.; Hurrell, E.; Bennett, K.; Congreve, M.; Magnani, F.; Tate, C. G.; Weir, M.; Marshall, F. H. Structure of the Adenosine A_{2A} Receptor in Complex with ZM241385 and the Xanthines XAC and Caffeine. *Structure* **2011**, *19*, 1283−1293.

(14) Jaakola, V. P.; Lane, J. R.; Lin, J. Y.; Katritch, V.; IJzerman, A. P.; Stevens, R. C. Ligand Binding and Subtype Selectivity of the Human A_{2A} Adenosine Receptor, Identification and Characterization of Essential Amino Acid Residues. *J. Biol. Chem.* **2010**, *285*, 13032−13044.

(15) Kim, J. H.; Jiang, Q. L.; Glashofer, M.; Yehle, S.; Wess, J.; Jacobson, K. A. Glutamate residues in the second extracellular loop of the human A_{2A} adenosine receptor are required for ligand recognition. *Mol. Pharmacol.* **1996**, *49*, 683−691.

(16) Lorber, D. M.; Shoichet, B. K. Flexible ligand docking using conformational ensembles. *Protein Sci.* **1998**, *7*, 938−950.

(17) Lorber, D. M.; Shoichet, B. K. Hierarchical docking of databases of multiple ligand conformations. *Curr. Top. Med. Chem.* **2005**, *5*, 739−749.

(18) Irwin, J. J.; Shoichet, B. K.; Mysinger, M. M.; Huang, N.; Colizzi, F.; Wassam, P.; Cao, Y. Q. Automated Docking Screens: A Feasibility Study. *J. Med. Chem.* **2009**, *52*, 5712−5720.

(19) Kuntz, I. D.; Chen, K.; Sharp, K. A.; Kollman, P. A. The maximal affinity of ligands. *Proc. Natl. Acad. Sci. U. S. A.* **1999**, *96*, 9997−10002.

(20) Hopkins, A. L.; Groom, C. R.; Alex, A. Ligand efficiency: a useful metric for lead selection. *Drug Discovery Today* **2004**, *9*, 430−431.
(21) Katritch, V.; Kufareva, I.; Abagyan, R. Structure based prediction of subtype-selectivity for adenosine receptor antagonists. *Neuropharmacology* **2011**, *60*, 108−115.